Korean J. Chem. Eng., 38(8), 1720-1726 (2021)
DOI: 10.1007/s11814-021-0811-7

pISSN: 0256-1115
eISSN: 1975-7220

Transparent Metal-Mesh heater using Silver-coated copper nanoparticles sintered with intense pulsed light irradiation on PET substrate

Soomin Song*, and Sung Min Cho*,†**

*School of Chemical Engineering, Sungkyunkwan University, Suwon 16419, Korea
**Semisysco, 94, Saneop-ro, Gweonseon-gu, Suwon 16643, Korea
(*Received 25 February 2021 • Revised 9 April 2021 • Accepted 14 April 2021*)

Abstract−A transparent metal-mesh heater was fabricated by intense pulsed light (IPL) sintering of copper-based particle ink on a polyethylene terephthalate (PET) substrate having a low glass transition temperature. The metal-mesh electrode with a line width of 9 μm was formed by filling imprinted intaglio patterns with silver-coated copper particle ink. This silver-coated copper particle is based on inexpensive copper and has excellent oxidation resistance as pure silver particle at temperatures up to 150 °C, making it suitable as a metal particle for metal-mesh heaters. This metal ink was IPL-sintered for the short time of 20 ms to obtain a transparent electrode with a low sheet resistance of 2 Ω/sq. without deterioration of the PET substrate. The silver thin film coated on the surface of the copper particles not only effectively blocks the reduction heat that may occur during the IPL sintering process, but also plays an important role in preventing the oxidation of copper during the operation of the transparent heater. It was confirmed that this flexible heater with 85% transparency is capable of stable operation up to 130 °C at a low voltage of 9 V.

Keywords: Intense Pulsed Light, Sintering, Transparent Electrode, Transparent Heater

INTRODUCTION

Transparent electrodes are important components widely used in fields such as displays [1] or solar cells [2]. Recently, as flexible devices have been developed and commercialized, their importance is gaining more attention. Indium-tin oxide (ITO) has been mainly used as a transparent electrode material, but various studies on alternative materials have been conducted to secure higher flexibility [3-5]. Examples of substitute materials for ITO include carbon nanotube, graphene, metal mesh, metal nanowires, or conductive polymers [6-11]. Among them, the metal-mesh transparent electrode is not only flexible, but also can be enlarged with low electrical resistance, so it is suitable for use in large- area flexible or wearable devices [12-14]. The metal-mesh transparent electrodes are formed by arranging metal materials such as copper or silver in a fine grid pattern which is made transparent by controlling the aperture ratio of the grid [15].

Typical metal-mesh transparent electrodes are expensive because they are manufactured by printing with expensive silver ink or etching copper foil by applying processes such as plating and photolithography [12,16-23]. Copper ink has been attracting attention to replace expensive silver ink because copper is only 20% of the price of silver and its electrical conductivity is about 90-95% [24,25]. Despite these advantages, copper has been limited in application because its surface oxidation easily occurs during sintering [26-28]. However, this shortcoming has been solved with the introduction of intense pulsed light (IPL) technology and active research is currently underway [29]. The IPL irradiation from Xenon lamp, which emits radiation in the wavelength range between 350 and 850 nm, enables sintering of metal particles within milliseconds under ambient conditions because the plasmon resonance bands of metal particles are in the visible spectrum [30]. Since this IPL sintering technology enables local heat treatment for a very short time, it is a technology that not only solves the problems of damage and deformation of the film substrate, but also increases cost competitiveness through continuous sintering process [31].

A metal-mesh transparent electrode can be utilized as a transparent heater because heat is generated when current flows at a certain voltage. Therefore, the metal-mesh electrode used for the transparent heater must be stable against oxidation at an elevated temperature [32,33]. Copper ink can be sintered through IPL irradiation, but when the sintered copper is used as a heating electrode, it is necessary to solve the problem of reoxidation [34]. Moreover, when copper particles whose surface is covered with a copper oxide film are sintered, heat is generated due to the reduction of the oxide. The reduction heat generated may cause cracks in printed metal patterns or substrates, which may lead to breakage of the electrode or permanent damage to the substrate [30,35,36]. This can be more serious when a substrate having a low glass transition temperature such as polyethylene terephthalate (PET) is used [35,37].

This study reports on a metal-mesh transparent heater that has low electrical resistance and excellent stability against oxidation at high temperature. To this end, the stability against oxidation and IPL sintering was evaluated using silver-coated copper nanoparticles on PET substrates. The silver layer on the surface of the copper particles effectively prevents the reoxidation of copper in the temperature range from 50 °C to 150 °C and the generation of reduction heat during IPL sintering process, enabling a low-cost transparent heater

†To whom correspondence should be addressed.
E-mail: sungmcho@skku.edu

on PET substrates. As a result, the silver-coated copper nanoparticle ink on PET substrates was IPL-sintered to fabricate and verify a metal-mesh heater that is stable even at 100 °C after heating. This transparent heater exhibits more improved properties than the commonly used ITO and silver-nanowire transparent heaters.

EXPERIMENTAL

As the metal particles for the metal ink, pure copper nanoparticles of two sizes (180 nm and 500-800 nm diameter, purchased from Guangbo, China) and copper nanoparticles (500 nm diameter) coated with silver were used. In the case of silver-coated copper particles which were purchased from JoinM (Korea), the silver content was 10%. A polyester resin (M_n=20,000, Needfill, Korea) was used as a binder for the metal nanoparticle ink and DISPERBYK-161 (BYK) was used as an additive for wetting and dispersion. Nanoparticle inks for IPL were formulated by mixing 0.4 g of polyester resin and 0.1 g of DISPERBYK-161 with 1.5 g of dipropylene glycol methyl ether solvent, and then mixing metal nanoparticles thereto. The mixed inks were dispersed for 1 hr using an ultrasonic mixer and then further dispersed using a three-roll mill.

After an ultra-violet (UV) curing resin was applied on a 125 μm-thick PET substrate, 9 μm-wide intaglio patterns were formed through an imprinting method. Metal nanoparticle ink was filled into the trench patterns using a doctor blade. During doctor-blading, the angle of the blade was maintained at 70° to minimize surface scratches and maximize the filling ratio of ink. Residual ink remaining around the intaglio patterns filled with metal ink was removed through a separate cleaning process and finally dried at 80 °C for 5 min to prepare a metal-mesh film.

The IPL sintering of the metal-mesh film involved an optical sintering system, myPET-AH430 (Semisysco, Korea) in the ambient conditions. This optical sintering system, which is composed of a Xenon lamp, a pulse power supply, and a lamp cooling chiller, is capable of evenly irradiating visible light in the wavelength range of 320-1,200 nm. For this experiment, the pulse duration and number of pulses were fixed at 20 ms and 1, respectively, and the irradiated light energy was controlled at 5-7.5 J/cm^2 by adjusting the voltage.

The heating characteristics of transparent heaters fabricated on PET film (50 mm×50 mm) were measured by applying a DC voltage through copper foils connected to the left and right sides of the film. When a voltage is applied through both terminals to pass an electrical current, heat is released by the resistance of the transparent electrode. Temperature rises and thermal images were measured with a thermal imaging camera (Fluke Co. Ltd., USA). The electrical resistance was measured with four-point probe using a source meter (Keithley 2400) after sintering the metal particles.

The surface microstructure of the sintered nanoparticle inks was analyzed with scanning electron microscopy (SEM, S4800 Hitachi) and electron dispersive X-ray spectroscopy (EDX) analyses to confirm the degree of oxidation during the sintering process. The inside of the sintered metal lines was cut using a focused ion beam (FIB, NOVA 600 Nanolab FEI) to analyze the cross-section. Light absorption of the sintered nanoparticle inks and optical transmittance of the transparent heaters were measured with a UV-visible spectrometer (UV-Vis, S-4100, SCINCO).

RESULTS AND DISCUSSION

Pure copper and silver-coated copper nanoparticle inks were printed on the polyimide (PI) substrate and subjected to IPL sintering. The printed line pattern was with a width of 1 mm and a length of 6.5 cm, and IPL sintering was performed with a single pulse for 20 ms with an energy of 7.5 J/cm^2 at a substrate temperature of 150 °C. It was confirmed that both inks were sufficiently sintered under this IPL sintering condition. For the sintered metal patterns to be utilized as a transparent heater, thermal stability at an elevated temperature is required. Therefore, the degree of oxidation at various temperatures for the IPL-sintered metal patterns using two inks was confirmed through SEM and EDX analyses.

After IPL sintering of the patterns printed with pure copper and silver-coated copper inks, the surface SEM images are almost similar to those of Figs. 1(a) and (e), respectively. When the sintered

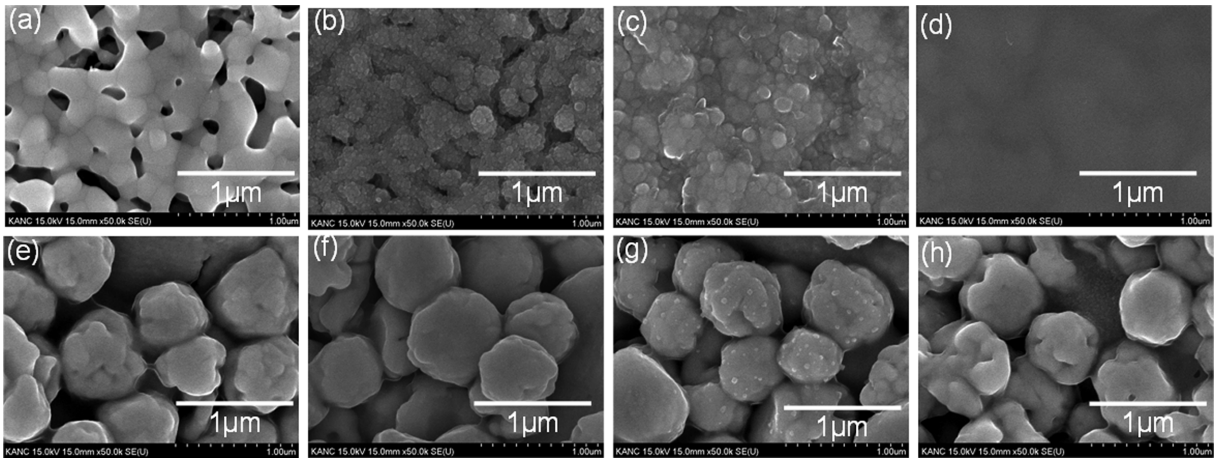

Fig. 1. SEM images of sintered pure copper particles on the PI substrate after aging for 24 hr at a temperature of (a) 25 °C, (b) 100 °C, (c) 150 °C, (d) 200 °C, and sintered silver-coated copper particles on the PI substrate after aging for 24 hr at (e) 25 °C, (f) 100 °C, (g) 150 °C, (h) 200 °C.

copper nanoparticles are aged for 24 hr at temperatures of 25, 100, 150, and 200 °C, the oxide film gradually covers the particles, and finally the particles cannot be distinguished. In contrast, in the case of silver-coated copper particles, almost no change in the oxidation state of the particles was observed even when aging was performed at elevated temperatures. To experimentally verify the degree of oxidation of the copper particles, the quantitative concentration of oxygen was measured by EDX analysis. As expected from the results of Fig. 1, in the case of pure copper nanoparticles, the concentration of oxygen atoms increased linearly with the increase of the aging temperature, but in case of silver-coated copper particles, only a moderate increase in oxygen concentration was observed above 150 °C. These results are shown in Fig. 2, and oxygen element mapping profiles are presented together in Fig. 3 for visual confirmation.

When the oxygen concentration increases as oxidation proceeds, the electrical resistance of the metal pattern increases. Fig. 4 shows the increase in resistance over time of pure copper and silver-coated

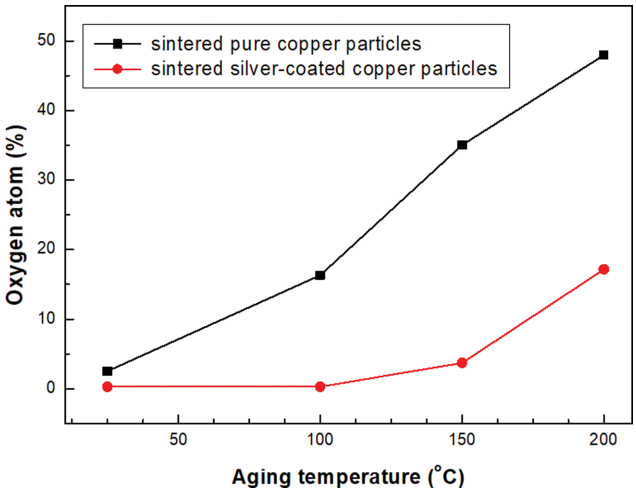

Fig. 2. Change of oxygen atom concentration in sintered particles with increasing aging temperature for 24 hr.

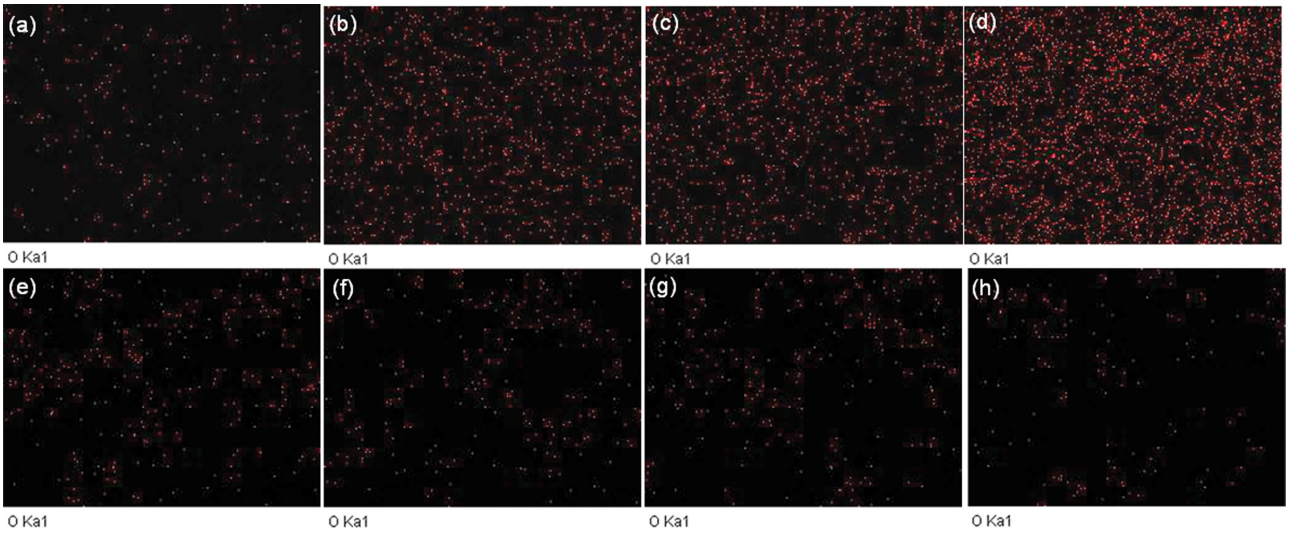

Fig. 3. Oxygen elemental mapping profiles of sintered pure copper particles on the PI substrate after aging for 24 hr at a temperature of (a) 25 °C, (b) 100 °C, (c) 150 °C, (d) 200 °C, and sintered silver-coated copper particles on the PI substrate after aging for 24 hr at (e) 25 °C, (f) 100 °C, (g) 150 °C, (h) 200 °C.

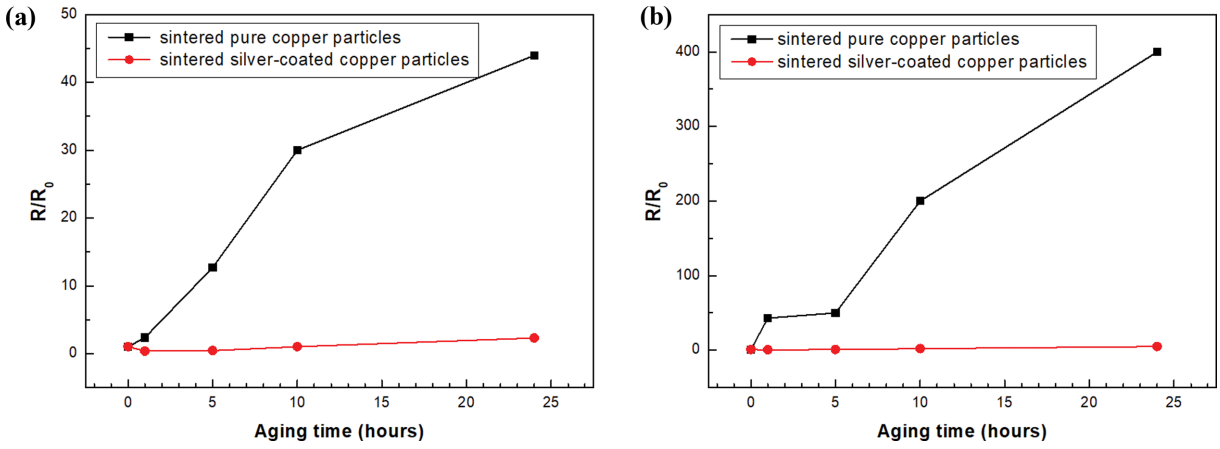

Fig. 4. Change in resistance-increase ratio (R/R_0) of sintered particles with aging time at (a) 100 °C and (b) 150 °C.

Table 1. Sheet resistance after sintering of various metal particles according to IPL sintering condition

Energy density (J/cm^2)	Heating condition (°C)	Sheet resistance of copper particle (180 nm) film (ohm/sq.)	Sheet resistance of copper particle (500 nm) film (ohm/sq.)	Sheet resistance of silver-coated copper particle film (ohm/sq.)	Sheet resistance of silver particle film (ohm/sq.)
5.5	-	∞	∞	20	3.4
6.5	-	∞	∞	18	3.3
7.5	-	∞	∞	17	3.1
7.5	80	∞	∞	8.0	3.0
7.5	100	∞	∞	2.4	2.3
7.5	120	∞	∞	1.5	1.6
7.5	150	damaged	damaged	damaged	damaged

copper nanoparticle patterns at aging temperatures of 100 and 150 °C. In case of pure copper nanoparticles, the resistance gradually increased with time and after 24 hr, the resistance increased 45 and 400 times compared to the initial resistance at temperatures of 100 and 150 °C, respectively. However, in the case of silver-coated copper particles, an increase in resistance was hardly observed. These experimental observations show that pure copper nanoparticles are not suitable for use as transparent heater electrode because oxidation easily occurs at an elevated temperature and eventually leads to an increase in resistance. As described above, it was confirmed that the silver-coated copper nanoparticles can be IPL-sintered at 150 °C on a PI substrate and have stability against oxidation even under high temperature conditions. To implement a transparent heater on a PET substrate using silver-coated copper nanoparticles, IPL sintering must be possible at a temperature lower than the glass transition temperature of PET. With this purpose in mind, IPL and/or low-temperature sintering process applicable to PET substrates was studied.

Using PET as a substrate, a transparent metal-mesh electrode was fabricated through low-temperature sintering to examine the possibility of use as a transparent heater. The experimental results are summarized in Table 1. In the case of pure copper nanoparticles, sintering hardly occurred even if the optical energy was increased without raising the substrate temperature, so that the resistance was measured indefinitely, and no improvement in electrical properties was observed even when thermal energy was additionally applied. This phenomenon was observed regardless of the size of the copper nanoparticles, because the energy for IPL sintering of pure copper particles is insufficient at the limited substrate temperature due to the use of PET substrate. On the other hand, in the case of silver-coated copper particles or pure silver particles, the resistance decreased as the optical energy increased. The initial resistance of silver-coated copper particles or pure silver particles was 20 and 3.4 Ω/sq., respectively, but when the optical energy for IPL sintering was gradually increased to 7.5 J/cm^2, the resistance decreased to 17 and 3.1 Ω/sq. If the substrate temperature is additionally increased to 120 °C while the optical energy is fixed, sufficient sintering is achieved in the case of silver-coated copper particles, and the resulting resistance is lowered similarly to that of pure silver particles. Increasing the substrate temperature to 150 °C damages the PET substrate in all cases.

When IPL is irradiated with sufficient energy on pure copper particles, oxidized copper on the surface of the particles undergoes chemical reduction due to reducing additives in the ink, resulting in sintering. In the case of pure copper particles, when IPL was irradiated with an energy of 7.5 J/cm^2 at a substrate temperature of 80-120 °C, it was expected that sufficient sintering would occur, but the resistance of printed copper lines was not measured. This may be because reducing heat generated during the sintering process caused damage to the substrate or printed copper lines. The effects of applied optical and thermal energy on the damage of the substrate or printed metal lines during the sintering process were evaluated for each metal particles and shown in Fig. 5. Figs. 5(a)-5(c) show the IPL sintering results according to the substrate temperature when the pure copper particle size is 180 nm. In the case of IPL sintering with an optical energy of 7.5 J/cm^2, cracks start to occur in the copper lines already when the substrate temperature is 80 °C. At a substrate temperature of 100 °C, cracks further expand and the empty space becomes larger. Finally, damage occurs to the substrate at 120 °C. When the pure copper particles are larger (500-800 nm), cracking is slightly delayed and occurs at a substrate temperature of 100 °C, and similarly, cracks propagate to the substrate at 120 °C. This result is shown in Figs. 5(d)-5(f). Cracks occur somewhat differently depending on the size of the copper particles. It can be understood that when the particle size is smaller, the generation of reduction heat increases due to an increase in the surface area where sintering occurs, and cracks occur at a lower substrate temperature due to the accumulated heat [38].

On the other hand, in the case of silver-coated copper particles, even if IPL sintering was performed while increasing the substrate temperature to 120 °C, the resistance continued to decrease as the sintering proceeded, but no damage to the substrate or metal lines occurred, as shown in Figs. 5(g)-5(i). This may be because the silver coated on the copper surface effectively prevented the oxidation of copper, so that the reduction heat of copper oxide was not released. To support these observations, the optical absorption of each metal particle was analyzed and shown in Fig. 6. In the case of pure copper particles, optical absorption occurs over a wavelength range of 300 to 850 nm, whereas in the case of pure silver or silver-coated copper particles, the absorption is much lower at a wavelength higher than 350 nm. The Xenon lamp used for IPL sintering emits light in the 350 to 850 nm wavelength range. The fact that pure copper particles with smaller sizes have greater absorption at wavelengths higher than 550 nm compared to larger parti-

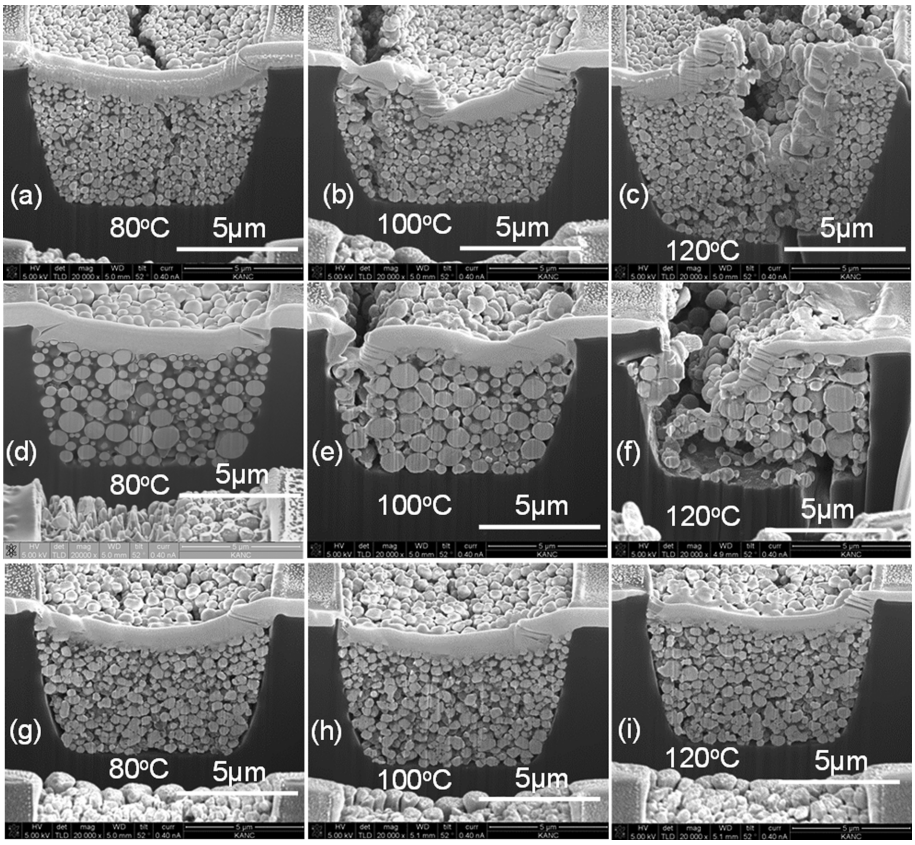

Fig. 5. Cross-sectional SEM images of 9 μm-wide IPL-sintered metal lines cut with focused ion beam. (a)-(c), (d)-(f), and (g)-(i) are pure copper (180 nm size), pure copper (500-800 nm size), and silver coated copper particles, respectively. The IPL sintering conditions were the same with a pulse duration time of 20 ms and a light energy of 7.5 J/cm^2 at each substrate temperature.

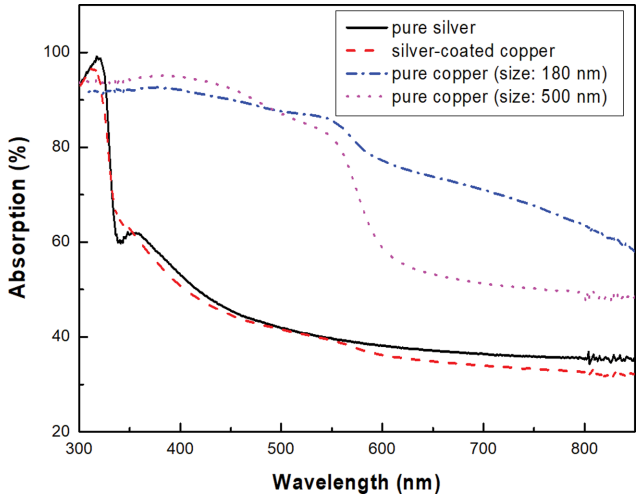

Fig. 6. Optical absorption spectra for various metal particle films.

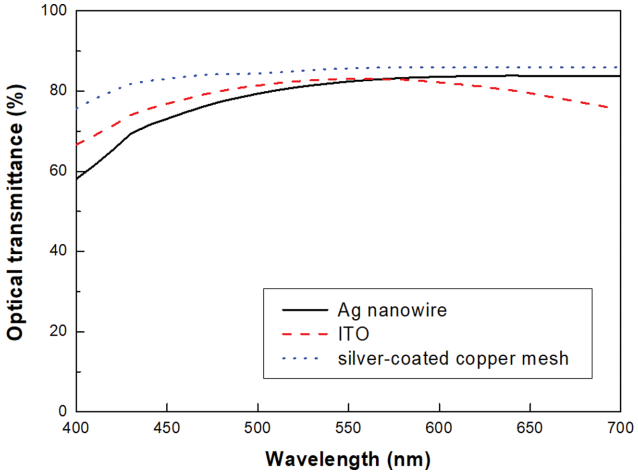

Fig. 7. Optical transmittance spectra of silver nanowire, ITO, and silver-coated copper particle mesh on PET substrates.

cles supports previous experimental results that the reduction heat generated by sintering is greater and damage is more prone to occur. Pure silver or silver-coated copper particles are relatively stable against damage because they absorb less light and do not generate reducing heat.

The previously mentioned results confirm that silver-coated copper particles have high stability against oxidation at high temperature; and even when applied to PET substrates, IPL sintering at low temperature can produce printed metal lines having electrical resistance equivalent to pure silver particles. A transparent metal-mesh heater was fabricated using this silver-coated copper particle ink, and the heater characteristics were compared with the case of

using the commonly used indium-tin oxide (ITO) and silver-nanowire electrode films. As shown in Fig. 7, the optical transmittance of the silver-coated copper mesh was 86% at a wavelength of 550 nm, which is the highest compared to that of ITO and silver-nanowire films. The sheet resistance of these heaters was 2, 11, and 10.2 Ω/sq. for silver-coated copper mesh, ITO, and silver nanowire films, respectively. Figs. 8(a) and 8(b) show the measured current and temperature of each heater according to the driving voltage. In the case of ITO and silver-nanowire heaters, the measured current and temperature follow similar trends due to similar resistance. In the case of silver-coated copper mesh heater, the slope of current increase with increasing voltage is much larger and the current flows about four times higher at the same voltage. In addition, the temperature of the metal mesh heater rose to 130 °C at a voltage of 9 V, whereas the ITO and silver-nanowire heaters were limited to within 70 °C. Fig. 8(c) shows thermal images taken with an infrared camera when voltage was applied to a silver-coated copper mesh heater. As shown in Figs. 8(c) and 9(a), the temperature of the silver-coated copper mesh heater rises to 100 °C at an applied voltage of 7 V, and this temperature is maintained stably for up to 600 s. As previously described, the temperature rise of ITO and silver-nanowire film heaters to 100 °C does not occur even at 9 V, but if the temperature is forcibly raised to 100 °C at a higher applied voltage, damage to the film occurs over time. When the heating temperature is set to 100 °C, the resistance of the ITO and silver-nanowire film heaters starts to increase from the initial resistance over time, and the resistance is no longer measured after 200 s. However, as shown in Fig. 9(b), the silver-coated copper mesh heater

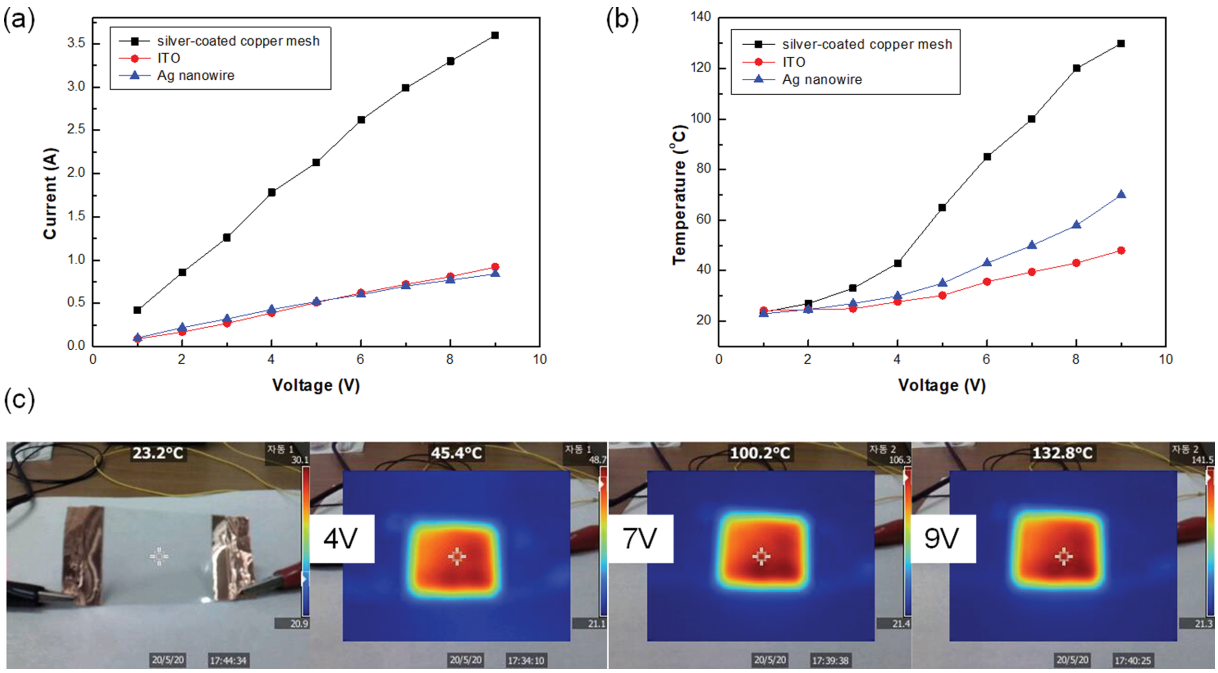

Fig. 8. (a) I-V characteristics and (b) temperature rise of transparent heaters during operation, (c) heating images of silver-coated copper mesh transparent heater at voltages of 4, 7 and 9 V.

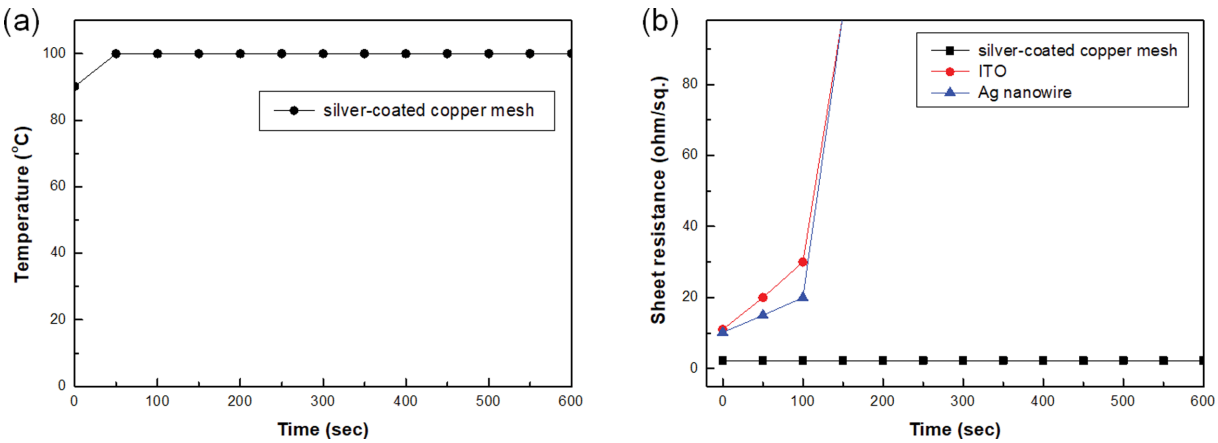

Fig. 9. (a) Temperature profile of silver-coated copper mesh at 7 V over time, (b) the change in sheet resistance over time when the heating temperature of transparent heaters is fixed at 100 °C.

maintains the initial sheet resistance of 2 Ω/sq. and is stable without any change even after 600 s. The thermal stability of this heater was further confirmed through a separate continuous operation experiment at 100 °C for 12 hours.

The results obtained from the above discussion are as follows. Low-resistance metal patterns can be formed through IPL sintering of pure copper nanoparticles, but when used as a transparent heater electrode, secondary oxidation occurs, resulting in poor thermal stability. As a complement to this problem, the use of silver-coated copper particles can ensure stability against oxidation, and electrical resistance equivalent to pure silver particles can be achieved through IPL sintering. The silver-coated copper mesh heater fabricated on PET substrate has low electrical resistance after IPL sintering and exhibits stable heating properties of 100 °C. This heater shows superior characteristics than the common ITO and silver-nanowire film heaters.

CONCLUSIONS

A metal-mesh heater was fabricated on PET substrate through IPL sintering. Mesh electrodes made of pure copper particle ink are vulnerable to oxidation when used as a heater, and cracks may occur in printed metal lines of PET substrate due to reduction heat generated during IPL sintering. These problems were solved by using silver-coated copper nanoparticles. Using these nanoparticles, stability against oxidation up to 200 °C can be secured and a low sheet resistance of 1.5 Ω/sq. on PET substrate can be implemented through 20 ms high-speed IPL sintering. Thanks to such low resistance and high temperature stability, this transparent heater is capable of stable heating operation up to 130 °C at voltage below 9 V. The transparent electrode using low-temperature IPL sintering of silver-coated copper nanoparticles can provide excellent competitiveness by lowering the material cost and process time.

REFERENCES

1. K. Watanabe, Y. Iwaki, Y. Uchida, D. Nakamura, H. Ikeda, M. Katayama, Takayuki. Cho, H. Miyake, Y. Hirakata and S. Yamazaki, *J. Soc. Inf. Display*, **24**, 12 (2016).
2. K.-T. Park, H.-J. Kim, M.-J. Park, J.-H. Jeong, J. Lee, D.-G. Choi, J.-H. Lee and J.-H. Choi, *Sci. Rep.*, **5**, 12093 (2015).
3. A. Kumar and C. Zhou, *ACS Nano*, **4**, 11 (2010).
4. D. S. Hecht, L. Hu and G. Irvin, *Adv. Mater.*, **23**, 1482 (2011).
5. S. Pang, Y. Hernandez, X. Feng and K. Müllen, *Adv. Mater.*, **23**, 2779 (2011).
6. J. Jang, *Mater. Today*, **9**, 46 (2006).
7. J.-Y. Lee, S. T. Connor, Y. Cui and P. Peumans, *Nano Lett.*, **8**, 689 (2008).
8. J.-W. Kim, S.-W. Lee, Y. Lee, S.-B. Jung, S.-J. Hong and M.-G. Kwak, *J. Nanosci. Nanotechnol.*, **13**, 6244 (2013).
9. D. J. Lipomi, J. A. Lee, M. Vosgueritchian, B. C.-K. Tee, J. A. Bolander and Z. Bao, *Chem. Mater.*, **24**, 373 (2012).
10. N. Cho, Y. Jung, K.-B. Chung and S. Kang, *Curr. Nanosci.*, **9**, 521 (2013).
11. K. Shin, R.-K. Park, L. Yu, C.-Y. Park, Y. S. Lee, Y.-S. Lim and J. H. Han, *Synth. Met.*, **161**, 1596 (2011).
12. S. Han, Y. Chae, J. Y. Kim, Y. Jo, S. S. Lee, S.-H. Kim, K. H. Woo, S. H. Jeong, Y. M. Choi and S. Y. Lee, *J. Mater. Chem. C*, **6**, 4389 (2018).
13. H. Y. Jang, S.-K. Lee, S. H. Cho, J.-H. Ahn and S. Park, *Chem. Mater.*, **25**, 3535 (2013).
14. B.-J. Kim, J.-S. Park, Y.-J. Hwang and J.-S. Park, *Thin Solid Films*, **596**, 68 (2015).
15. H. Nam, D. Seo, H. Yun, G. Thangavel, L. Park and S. Nam, *Metals*, **7**, 176 (2017).
16. Y. Horiuchi, Y. Suzuki, J.-H. Noh, H. Honma, O. Takai and C. E. J. Cordonier, *Electrochemistry*, **84**, 971 (2016).
17. X. Zhang, Y. Pan, J. Zhao, X. Hao, Y. Wang, D. W. Schubert, L. Liu, C. Shen and X. Liu, *Engineered Science*, **7**, 65 (2019).
18. W. Zhou, J. Chen, Y. Li, D. Wang, J. Chen, X. Feng, Z. Huang, R. Liu, X. Lin, H. Zhang, B. Mi and Y. Ma, *ACS Appl. Mater. Interfaces*, **8**, 11122 (2016).
19. O. S. Hutter, H. M. Stec and R. A. Hatton, *Adv. Mater.*, **25**(2), 284 (2012).
20. D.-J. Kim, H.-J. Kim, K.-W. Seo, K.-H. Kim, T.-W. Kim and H.-K. Kim, *Sci. Rep.*, **5**, 1 (2015).
21. R. Dharmadasa, M. Jha, D. A. Amos and T. Druffel, *ACS Appl. Mater. Interfaces*, **5**, 13227 (2013).
22. P. Xu and M. C. Hamilton, *IEEE Microw. Wirel. Compon. Lett.*, **23**(4), 178 (2013).
23. Y. Han, H. Zhong, N. Liu, Y. Liu, J. Lin and P. Jin, *Adv. Electron. Mater.*, **4**, 1800156 (2018).
24. S. Jang, Y. Seo, J. Choi, T. Kim, J. Cho, S. Kim and D. Kim, *Scr. Mater.*, **62**, 258 (2010).
25. B.-Y. Wang, T.-H. Yoo, Y.-W. Song, D.-S. Lim and Y.-J. Oh, *ACS Appl. Mater. Interfaces*, **5**, 4113 (2013).
26. M. S. Rager, T. Aytug, G. M. Veith and P. Joshi, *ACS Appl. Mater. Interfaces*, **8**, 2441 (2016).
27. H.-J. Hwang, W.-H. Chung and H.-S. Kim, *Nanotechnology*, **23**, 485205 (2012).
28. M. Joo, B. Lee, S. Jeong and M. Lee, *Thin Solid Films*, **520**(7), 2878 (2012).
29. J. Ryu, H.-S. Kim and H. T. Hahn, *J. Electron. Mater.*, **40**, 42 (2010).
30. W.-H. Chung, Y.-T. Hwang, S.-H. Lee and H.-S. Kim, *Nanotechnology*, **27**, 205704 (2016).
31. H.-J. Hwang, K.-H. Oh and H.-S. Kim, *Sci. Rep.*, **6**, 1 (2016).
32. J. Park, D. Han, S. Choi, Y. Kim and J. Kwak, *RSC Adv.*, **9**, 5731 (2019).
33. L. Veeramuthu, B.-Y. Chen, C.-Y. Tsai, F.-C. Liang, M. Venkatesan, D.-H. Jiang, C.-W. Chen, X. Cai and C.-C. Kuo, *RSC Adv.*, **9**, 35786 (2019).
34. J. Perelaer, B.-J. DeGans and U. S. Schubert, *Adv. Mater.*, **18**, 2101 (2006).
35. X. Chen, X. Wu, S. Shao, J. Zhuang, L. Xie, S. Nie, W. Su, Z. Chen and Z. Cui, *Sci. Rep.*, **7**, 1 (2017).
36. W. Li, D. Hu, L. Li, C.-F. Li, J. Jiu, C. Chen, T. Ishina, T. Sugahara and K. Suganuma, *ACS Appl. Mater. Interfaces*, **9**, 24711 (2017).
37. X. Wu, S. Shao, Z. Chen and Z. Cui, *Nanotechnology*, **28**, 035203 (2016).
38. W. Macneill, C.-H. Choi, C.-H. Chang and R. Malhotra, *Sci. Rep.*, **5**, 1 (2015).